Optics Communications 516 (2022) 127945

Contents lists available at ScienceDirect

Optics Communications

journal homepage: www.elsevier.com/locate/optcom

The formation of transient defects during high power laser-coating interaction revealed by the variation of electron beam evaporated coatings' optical constants with temperature

Kaixin Zhang [a,b,c,1], Xiaoyan Wang [a,b,c,1], Jianda Shao [a,c,d,e,*], Kui Yi [a,c,d,*], Yigu Hu [a,b,c], Guohang Hu [a,c,d], Maria Luisa Grilli [f], Yingjie Chai [g]

[a] Laboratory of Thin Film Optics, Shanghai Institute of Optics and Fine Mechanics, 390 Qinghe Road, Jiading District, Shanghai 201800, China
[b] Center of Materials Science and Optoelectronics Engineering, University of Chinese Academy of Sciences, Beijing 100049, China
[c] Key Laboratory of Materials for High Power Laser, Chinese Academy of Sciences, Shanghai 201800, China
[d] CAS Center for Excellence in Ultra-intense Laser Science, 390 Qinghe Road, Jiading District, Shanghai 201800, China
[e] Hangzhou Institute for Advanced Study, University of Chinese Academy of Sciences, Hangzhou 310024, China
[f] Energy Technologies and Renewable Sources Department, Italian National Agency for New Technologies, Energy and Sustainable Economic Development (ENEA), Via Anguillarese 301, 00123 Rome, Italy
[g] CREOL, The College of Optics and Photonics, University of Central Florida, Orlando, FL 32816, USA

ABSTRACT

The knowledge of the optical properties of coating materials at high temperatures is important for understanding the dynamic process of high-power laser-material interactions. In this paper, the variations of refractive index and physical thickness of single layer coatings were studied by ellipsometric spectroscopy at different temperatures. From 23 °C to 320 °C, a decrease and then an increase of the refractive index of SiO_2, and HfO_2 single layer was observed, while the thickness of these layers increased first and then decreased. The inflection points of different coating materials occurred at different temperatures. Water evaporation processes, densification and hydrophilicity of films were used to explain the temperature dependent properties of the dielectric coatings. Results of the variation of refractive index and thickness of single layer coatings at different temperatures in the vacuum proved the mentioned theory. Moreover, HfO_2 single layer shows better resistance to both temperature change and vacuum change, indicating that it is promising for high-reflective coatings in photoelectric devices. Besides, the formation of transient defects during high power laser irradiation was interpreted considering the optical properties variation with temperature. Three confusing and debated issues concerning laser-coating interaction are interpreted and explained.

1. Introduction

Optical coatings, such as high-reflective coatings [1,2], anti-reflective coatings [3], and polarizers [4], are essential components in laser systems. Besides, optical films are the most fragile parts in high-power laser system for their low laser-induced damage threshold (LIDT) [5]. Therefore, laser induced damage [6] or thermal distortion of films [7] under high-power laser irradiation limits the development of high-power laser technology.

Although laser-induced damage of optical coatings has been studied over the past five decades [7–11], researchers still encounter several confusing problems both in pulse laser system and continuous-wave (CW) laser system. First, the UV LIDT of the coating deposited by electron-beam technique is much lower than the infrared LIDT [12]. For example, when a 200 nm-thick alternative HfO_2/SiO_2 film, for which the thickness of HfO_2 layer is 40 nm and that of SiO_2 layer is 57 nm, is exposed to a 1000-shot laser pulse with a duration of 12 ns and a diameter of 195 μm, the laser fluence of LIDT at the irradiation wavelength of 355 nm is only 10 J/cm^2, and that at 1064 nm can reach >150 J/cm^2. The photon energy at 355 nm is three times that of 1064 nm, but the LIDT at 1064 nm is much larger than 3 times the LIDT at 355 nm. Second, the coupling mechanism of substrate and coating is not clear. The LIDTs of the same optical coating deposited on different substrates are different, and lower than that of the uncoated substrate. For example, when illuminated by an ultrashort femtosecond (fs) laser pulse with a duration of 500 fs, a wavelength of 1030 nm, and a diameter of around 70 μm, the laser fluence of LIDT of fused silica is 4.6 J/cm^2 [13], and the laser fluence of LIDT of a 247 nm-thick TaO_2 single layer film on the fused silica is 1.0 J/cm^2 [14].

For a CW regime with a wavelength of 1064 nm and a spot size of 20 μm, the power density of LIDT of a fused silica substrate with the exposure time of 6 s was 250 kW/cm^2, while that of LIDT of a 60 nm-thick titania deposited on the fused silica substrate with the same 6 s-exposure time is 80 kW/cm^2 [15]. Third, the LIDT of coatings

* Corresponding authors at: Laboratory of Thin Film Optics, Key Laboratory of Materials for High Power Laser, Shanghai Institute of Optics and Fine Mechanics, Chinese Academy of Sciences, Shanghai, 201800, China.
E-mail addresses: jdshao@siom.ac.cn (J. Shao), kyi@siom.ac.cn (K. Yi).
[1] Kaixin Zhang and Xiaoyan Wang contributed equally to this work.

https://doi.org/10.1016/j.optcom.2022.127945
Received 12 October 2021; Received in revised form 10 December 2021; Accepted 10 January 2022
Available online 17 January 2022
0030-4018/

in the vacuum is lower than that in the atmosphere. When irradiated by a 7.6 ns duration laser pulse with a wavelength of 355 nm and a diameter of 1.0 mm, the laser fluence of LIDT of a 5 cm diameter fused silica substrate in the vacuum of 10^{-6} Torr is 20 J/cm^2, which is 10 J/cm^2 lower than the value of 30 J/cm^2 in the air [16]. Therefore, it is important to deeply study what changes occur in the coating and on the substrate during the laser irradiation process, so as to fundamentally reveal the damage mechanism.

The laser-coating interaction involves a thermal process, no matter in a continuous-wave laser system or a pulse laser system [7,17–19]. The irradiated optical coatings absorb laser energy, and the temperature of the irradiated region increases, leading to the change of optical constants and thickness of coatings. The change of parameters of a film will make it exposed to an external force, which is a key to the laser-induced damage of coatings. Therefore, understanding and measuring the variation of optical properties and physical properties of coatings with temperature is important to reveal the dynamics of the laser damage process.

Ellipsometry with ultra-high sensitivity is an effective way to determine the optical constants and thickness of thin films. Recently, with the development of variable-temperature ellipsometry technology, the temperature dependence of optical constants has attracted considerable attention [20,21] due to its wide application in studies of thermal expansion, electronic band structures [22,23] and phase transitions [24–26]. Therefore, measuring parameters of coatings by ellipsometry can be accurate and with high sensitivity.

In this paper, we reported on a study of the variation of the refractive index and the physical thickness of SiO_2, and HfO_2 single layer films, and the BK7 substrate with temperature and vacuum. These two kinds of representative optical dielectric materials, SiO_2, and HfO_2 with different hydrophobic and hydrophilic performance, are widely used in high-power laser systems [27]. The changes of refractive index and optical thickness of these layers with temperature both in the atmosphere and in the vacuum were measured, and the changes in the optical properties of the coatings were analyzed. The optical constant of the BK7 showed a low variation with temperature. It was also observed that the refractive index of SiO_2, and HfO_2 single layer films decreased firstly and then increased was observed, while the thickness of these layers increased first and then decreased. Water evaporation processes, densification and hydrophilicity of films are used to elucidate the different inflection points of SiO_2, and HfO_2 single layer films. In order to fully prove the proposed explanation, the property change of films with temperature in the vacuum was also studied. In the vacuum, it was found that a drastic decrease of the refractive index of SiO_2 and HfO_2 at the wavelength of 532 nm and an increase of thickness when the atmospheric pressure changed into the vacuum pressure. It results from the water loss in the pores and adhering of escaping water and organic contaminants. The measurement in the vacuum can be also used to study the laser-coating interaction in the vacuum, which can be applied to the space science. Based on these results, the formation of transient defects in optical coatings during high power laser irradiation was revealed, and the dynamic of laser damage process was discussed. The laser-coating interaction was discussed and interpreted by three examples, including alternative SiO_2/HfO_2 multilayer layers, coating-substrate coupling and the lower LIDT of film in the vacuum. Different behaviors of different films and substrate with temperature lead to a stress in the interface of alternating SiO_2/HfO_2 multilayer layers, and in the interface of the coating and the substrate. This reveals that the laser-induced damage easily forms in the interface, and the lower LIDT of a coating than the uncoated substrate. In the vacuum, an abrupt and different change of SiO_2 and HfO_2 single layer films, leading to a stress in the interface of multilayer coatings, and vacuum organic contamination are essential to the lower LIDT of film in the vacuum than in the atmospheric pressure [16].

2. Materials and methods

2.1. Film preparation

In the experiment, SiO_2 and HfO_2 single layer with a thickness of ~200 nm were deposited on the BK7 substrate by electron beam evaporation (EBE), which is a common preparation technique of dielectric coatings for laser applications. The sources are SiO_2 powders (Umicore, 99.99% purity) and Hf granules (Merk KGaA, 99.99% purity), respectively. The diameter of the substrate was 30 mm and its thickness was 3 mm. Prior to deposition, substrates were submitted to a cleaning procedure in acetone and isopropyl alcohol. Samples were fabricated by a Leybold Syrus Pro e-beam deposition system. The deposition temperature is 200 °C, and the Oxygen partial pressures are 1.4×10^{-2} Pa for HfO_2 single layer, and 5×10^{-3} Pa for SiO_2 single layer, respectively. The distance between the substrate and the evaporator is 70 cm. The deposition rates are 0.14 nm/s for HfO_2, and 0.6 nm/s for SiO_2 single layer, respectively. During the coating time, the substrate of HfO_2 was kept still, while the substrate of SiO_2 rotated at a low rate of 0.1 rpm. After deposition, the atom contents were measured by X-ray photoelectron spectroscopy (XPS) to prove that films were fully stoichiometric.

2.2. Experimental setup and theoretical calculation

The experimental setup is shown in Fig. 1. In order to measure the variation of the thickness and the optical constants of coatings at different temperatures under atmospheric pressure or in the vacuum, a Horiba UVISEL-2 ellipsometer was used. The heating stage of Linkam THMS350V System was used to heat the samples to different temperatures, in the range from 23 °C to 320 °C. A pump on one side of the heating stage was used to change the ambient pressure from the atmosphere to 0.1 Pa. The windows of the sealing cover were perpendicular to the linearly polarized light beam, so the direction of the incident light beam was not changed. The ellipsometry measuring angle was 70°. The humidity was controlled to ~40%.

Ellipsometric parameters Ψ and Δ are defined by a complex ratio (ρ) of the p- and s-polarized Fresnel reflection coefficients r_p and r_s, respectively, which is given by,

$$\frac{r_p}{r_s} = tan(\Psi)\, e^{i\Delta} \tag{1}$$

the refractive index n and the thickness d of the singer layer are calculated from the Ψ and Δ.

During the experiment, the heating stage was in contact with the back of the sample, as shown in Fig. 1. In order to keep the temperature at the surface of the coating stable, the heating system continued working for 30 min after reaching the preset temperature. The temperature range was set from 23 to 320 °C, wavelength range was set from 400 nm to 800 nm, and the dielectric layer was modeled using the classical dispersion formula [28]: $\tilde{\varepsilon}(\omega) = \varepsilon_\infty + \frac{(\varepsilon_s - \varepsilon_\infty)\cdot\omega_t^2}{\omega_t^2 - \omega^2 + i\cdot\Gamma_0\cdot\omega}$, where $\varepsilon_\infty = 1$ eV is the high frequency dielectric constant, $\varepsilon_s = 2.5$ eV is the static dielectric function at a zero frequency, $\Gamma_0 = 5$ eV is the damping factor of the single Lorentz oscillator, $\omega_t = 12$ eV is the resonant frequency of the oscillator whose energy corresponds to the absorption peak. The optical constants of the coatings were obtained by modeling the spectral dependences of Ψ and Δ, and minimizing the χ^2 values [29]. As shown in Fig. 2, the χ^2 value is a comparison of theoretically calculated pairs (Ψ_{th}, Δ_{th}) and experimentally determined pairs (Ψ_{exp}, Δ_{exp}),

$$\chi^2 = min \sum_{i=1}^{n} \left[\frac{(\psi_{th} - \psi_{\exp})_i^2}{\Gamma_{\psi,i}} + \frac{(\Delta_{th} - \Delta_{\exp})_i^2}{\Gamma_{\Delta,i}} \right] \tag{2}$$

where $\Gamma_{\Psi,i}$ and $\Gamma_{\Delta,i}$ are the standard deviations of experimental ellipsometric parameters Ψ_{th} and Δ_{th}, respectively. The goodness of fit is determined by the χ^2 value which should be as low as possible. In this experiment, χ^2 was less than 0.5.

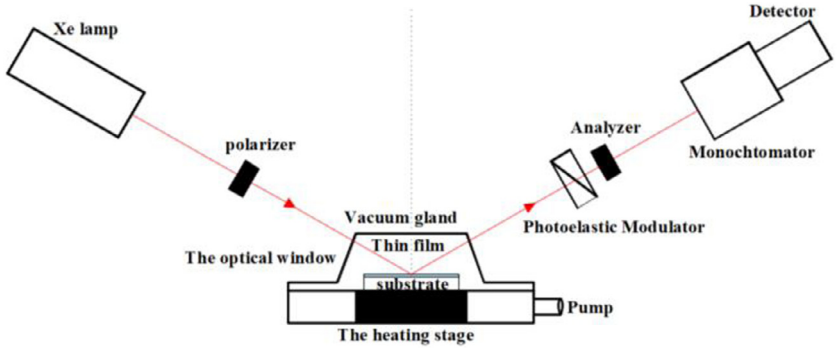

Fig. 1. Optical path to measure ellipsometric parameters of thin films under heating at different temperatures.

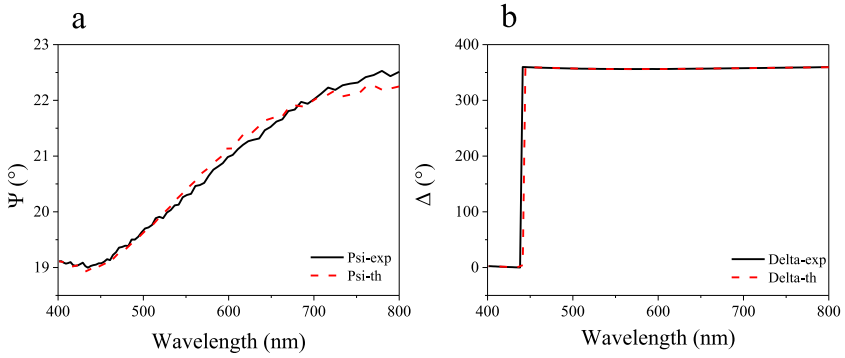

Fig. 2. Experimental and theoretical ellipsometric parameters of (a) Ψ and (b) Δ of the SiO_2 single layer under atmospheric pressure at 23 °C.

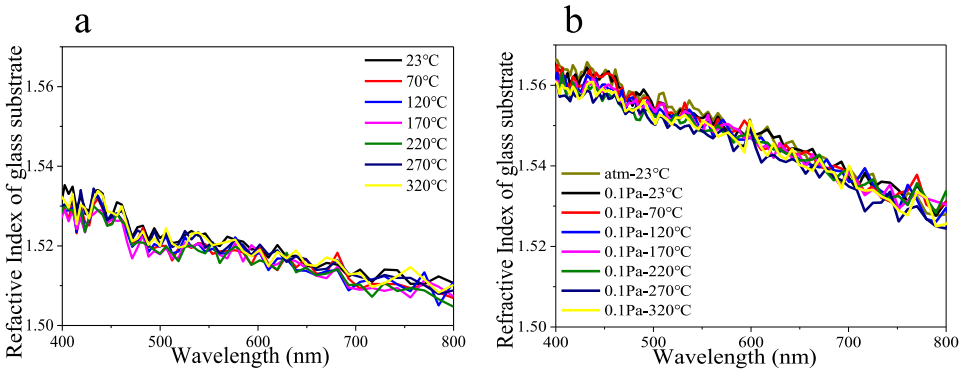

Fig. 3. Variation of refractive index of the BK7 glass substrate with temperature (a) under atmospheric pressure and (b) in vacuum environment.

3. Results

3.1. Variation of substrate optical constants at different temperatures

The refractive index of the BK7 glass substrate was measured at different temperatures. Ellipsometric measurements were made at increments of every 50 °C from 23 °C to 320 °C. The measuring results are shown in Fig. 3, which shows that temperature and pressure changes have a small effect on the refractive index of the BK7 glass in the selected temperature range.

3.2. Variation of the thickness and the refractive index of coatings at different temperatures under atmospheric pressure

Figs. 4–5 show the variation of the refractive index and the thickness of SiO_2 and HfO_2 single layer films with temperature ranging from 23 °C to 320 °C under atmospheric pressure. In Fig. 4, the refractive index of the SiO_2 coating at 532 nm decreases by 3.2% with temperature changing from 23 °C to 270 °C and then increases by 0.4% from 270 °C to 320 °C. The thickness of the SiO_2 coating increases by 4.1% firstly and then decreases by 4.0% from 170 °C to 320 °C.

As shown in Fig. 5, the variation of the refractive index and the thickness of the HfO_2 coating with temperatures shows the same trend. But the temperature of the turning point of the SiO_2 coating is higher than that of the HfO_2 coating. For the HfO_2 coating, the temperatures of the turning points of the refractive index and the thickness are 220 °C and 120 °C, respectively. The refractive index at 532 nm decreases by 2.9% in the temperature range from 23 °C to 170 °C. From 170 °C to 320 °C, the refractive index increases by 0.4%. Corresponding to the variation of refractive index, the thickness rises by 0.5% as the temperature increases from 23 °C to 120 °C, and decreases by 1.0% from 120 °C to 320 °C. Overall, the two kinds of materials are ranked by the temperature turning points of the refractive index and the thickness as follows: SiO_2 > HfO_2. According to the change amount in refractive index and thickness, they are also sorted in the same order. The HfO_2 single layer is more resistant to the change of temperature.

In the first stage of the heating process, the decrease of refractive index is mainly because of the water loss in the films, and the increase

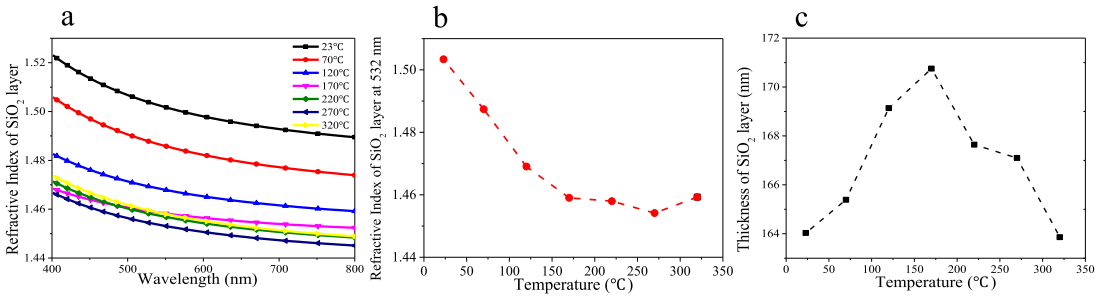

Fig. 4. Variation of (a) refractive index, (b) refractive index at 532 nm, (c) thickness of SiO_2 layer at different temperatures under atmospheric pressure.

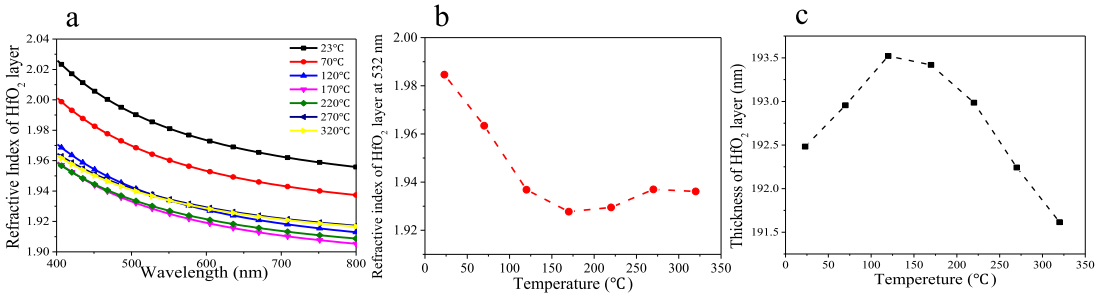

Fig. 5. Variation of (a) refractive index, (b) refractive index at 532 nm and (c) thickness of HfO_2 layer at different temperatures under atmospheric pressure.

of the thickness is greatly due to the expansion of water adhering on the surface of the films. The film microstructure consists of columnar structures, with voids between columns [30]. The refractive index of the air in the void is 1.0, but it changes to 1.333 when the void is filled with water after moisture absorption. Therefore, in the heating process, the water vaporizes from the liquid to gas continuously as the temperature rises, and therefore the refractive index of SiO_2 and HfO_2 coatings decreases [31]. The optical thickness of films can be expressed as [30],

$$n \cdot d = n_{layer} \cdot d_{layer} + n_{vapor} \cdot d_{vapor} \tag{3}$$

where n_{layer} is the refractive index of a film without adsorbate, d_{layer} is the thickness of a film without adsorbate, n_{vapor} is the refractive index of adsorbate vapor, and d_{vapor} is the thickness of the adsorbate vapor. It has been confirmed that the Si-OH groups are abundant on the surface of the SiO_2 coating, and that the water is chemically bonded with the SiO_2 coating [32,33]. The water vapor, which evaporates from the voids, accumulates on the surface of the film and constantly expands upon heating, which leads to the increase of the film thickness.

The densification of annealing is regarded to dominate the second stage of the heating process with the refractive index increasing and the thickness decreasing. As the temperature increases, water remaining in the void decreases. When the remaining water is negligible, the densification of annealing plays a vital role. The surface energy of voids is larger than that of grain boundary [34]. Therefore, the voids tend to shrink, and the films become denser. So the refractive index begins increasing and the thickness decreasing.

SiO_2 is hydrophilic due to the surface OH groups [35], while HfO_2 is usually hydrophobic [36]. Water vapor is more tightly attached to the surface of the SiO_2 film. Therefore, the temperature of the turning point and the change amount of the SiO_2 film is higher than that of HfO_2 films.

3.3. Variation of the thickness and the refractive index of coatings at different temperatures in the vacuum

In order to further verify the influence of water loss, densification and hydrophilicity on refractive index and thickness of coatings, the variation of the refractive index and thickness of SiO_2 and HfO_2 coatings with temperature were measured also in a vacuum. Figs. 6 and 7 show the variation of the refractive index and the thickness of SiO_2 and HfO_2 single layer films with temperatures ranging from 23 °C to 320 °C in the vacuum. When the ambient pressure changes from the atmosphere to 0.1 Pa, the refractive index of SiO_2 and HfO_2 at 532 nm decreased by 2.0% and 1.6%, respectively, while the thickness increased by 3.4% and 0.3%, respectively. As the temperature continues to increase at 0.1Pa, the refractive index of SiO_2 and HfO_2 continues to decrease by 0.3% and 1.1%, respectively. While the thickness of SiO_2 decreased by 0.8%, the thickness of HfO_2 firstly increases by 0.2% from 23 °C to 220 °C and then decreases by 0.5% from 220 °C to 320 °C. It suggests that the ambient pressure change plays a more vital role in the variation of the thickness and the refractive index of coatings than the temperature change. Overall, when the pressure changes, the variation amount of refractive index and thickness are orderly sorted by SiO_2 > HfO_2, respectively. The pressure has a larger effect on the SiO_2 film. When the temperature rises, the order of change amount of refractive index is HfO_2 > SiO_2. When it comes to the thickness of films, the two materials show a different trend. The thickness of SiO_2 decreases, and that of HfO_2 increases and then decreases. The order of the temperature of the turning points can be seen as HfO_2 > SiO_2. They are listed in order of the change amount is thickness as SiO_2 > HfO_2. It suggests that the HfO_2 single layer is more stable when the pressure changes.

When the pressure changes from the atmosphere to 0.1 Pa, the water in the pores of the coating escapes during the pumping process, and the refractive index of the pores changes from 1.33 to 1.0, which causes the refractive index of the coating to drop rapidly. However, the effect of air-vacuum is still related to the hydrophilicity of the material. SiO_2 is hydrophilic, while HfO_2 is hydrophobic. The SiO_2 coating is filled and bonded with more water than the HfO_2 coating, so the refractive index of SiO_2 coating is strongly affected by vacuum. The air-vacuum change also results in the adsorption of organic contaminants [37], such as di-butyl-phthalate (DBP) and Paraffin-oil. These contaminants come from steel parts and mechanical parts of the vacuum chamber. The escaping water and organic contamination adhere to the surface of films by hydrogen bonding with the OH group [38,39], leading to the sharp increase of thickness of films. The moisture of SiO_2 single

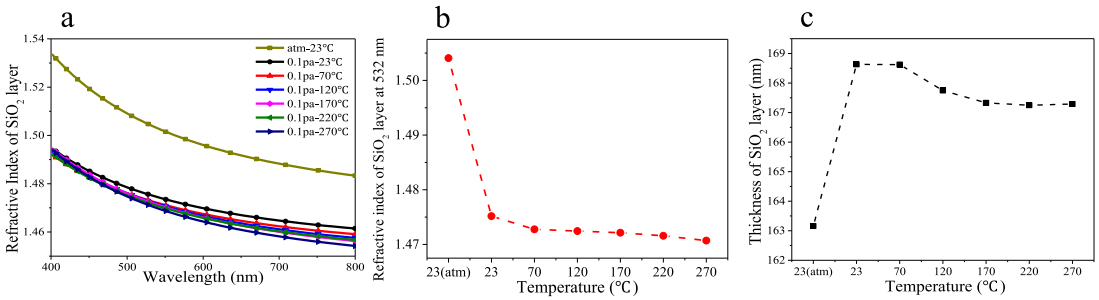

Fig. 6. Variation of (a) refractive index, (b) refractive index at 532 nm, and (c) thickness of SiO_2 with temperature in vacuum.

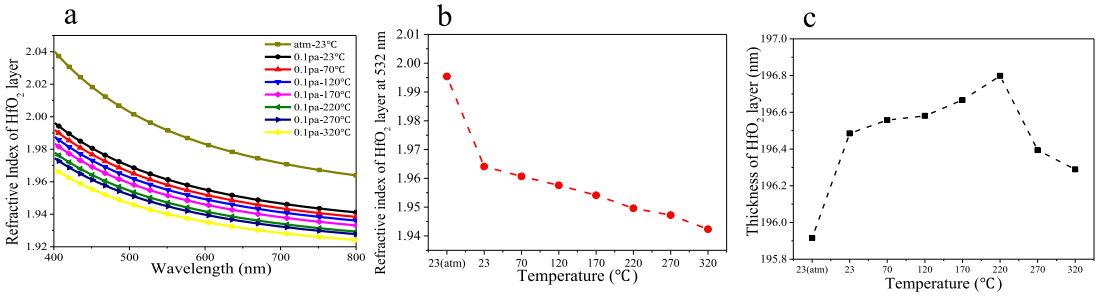

Fig. 7. Variation of (a) refractive index, (b) refractive index at 532 nm and (c) thickness of HfO_2 with temperatures in vacuum.

layer makes it more attractive to the organic contaminants, which is the reason that the thickness of SiO_2 increases more obviously [40].

As the temperature continues to increase at 0.1 Pa, it is suggested that the distance between organic molecules increases, resulting in the decrease of refractive index and the increases of the thickness of the HfO_2 coating. When the temperature is high enough to break Hf-OH bonds, the organic contaminants release from the surface and the densification of films plays a vital role, so the thickness of HfO_2 films decreases. However, the energy of the Si-OH bond is smaller, and therefore, the constitutional water and organic molecules in SiO_2 can be easily removed and the thickness decreases as the temperature increases. There is no airflow in the vacuum so that the organic contamination remains on the surface [37]. This is the reason why the thickness of SiO_2 and HfO_2 in the vacuum decrease more slowly than that in the atmospheric pressure.

4. Discussions

As described above, SiO_2 and HfO_2 single layer films, and the glass substrate have different behaviors with temperature and vacuum. As shown in Eq. (4), the variations of optical constants of coatings generates a stress.

$$\varepsilon = \frac{dI}{I_0} = \frac{\sigma}{E} \tag{4}$$

where ε is the strain, σ is the stress, E is the Young's modulus, I_0 is the original length, dI is the change of length. When an optical multilayer coating used in the high-power laser system, such as lenses and the mirrors, it is inevitably involved in a thermal process, and generates a thermal stress. Therefore, the different behaviors of two kinds of layers like SiO_2 and HfO_2 in the multilayer coating led to a stress in the interface, which is vulnerable to the laser irradiation. It is the same for a single layer coating evaporated on a stable substrate.

4.1. Laser-induced defects at/near the interface of different coatings

For a multilayer $(HL)^{10}H4L$ coating, where H denotes the HfO_2 layer with a thickness of 134.0 nm, and L denotes SiO_2 layer with a thickness of 183.4 nm, as shown in Fig. 8. When exposed to a 1064 nm laser with a duration of 8 ns and a fluence of ~23.5 J/cm^2, most of nano-holes are formed at the interface. The curve at the damage site proves that there exists tensile stress. Therefore, a damage precursor is easier to be formed at the interface of the two different coatings, due to the different behavior of the two layers while they are irradiated by high-power laser. These defects become the precursor of laser induced damage. The formation of point damage at or near the interface prove that transient defects could be formed during laser-material interaction. About the fact that the IR LIDT is much larger than 3 times the UV LIDT [12], the transient defects should also be considered. Due to the different behavior of the high-index coating, low-index coating and the substrate at high temperature, transient defects form during high power laser irradiation. Transient defects have a band gap smaller than the photon energy of UV laser, but larger than the photon energy of IR laser [41,42]. Therefore, damage happens easier during the UV radiation.

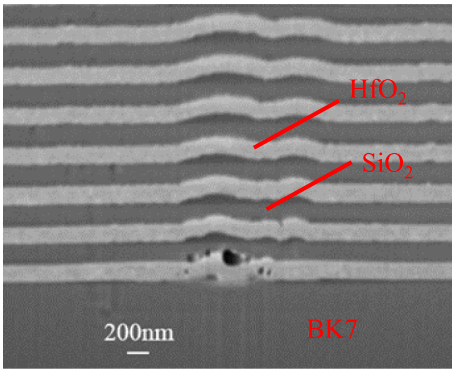

Fig. 8. The cross-sectional SEM micrograph of laser induced damage in a HfO_2/SiO_2 stack, irradiated by a laser pulse. The bright pattern is the HfO_2 layer, the dark pattern is the SiO_2 layer, and the bottom dark part is the BK7 substrate.

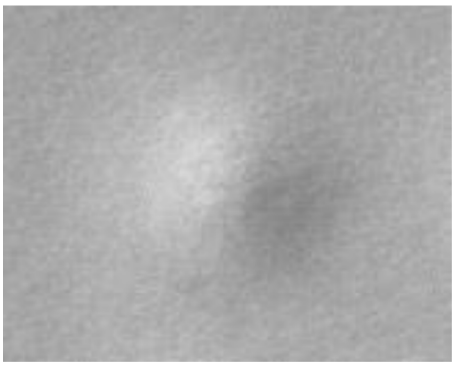

Fig. 9. Bulging of a Au-SiO_2-Au coating under laser irradiation.

4.2. The different behavior between coatings and substrate with laser irradiation

About the coupling mechanism of the substrate and the coating during high power laser irradiation, the large different behavior of the substrate and the coating material at different temperature should be considered. According to our experimental results, when the temperature increases, the properties of some substrate changes very little, while the thickness and refractive index of the coating change a lot. There is a tensile stress between the coating and the substrate. When the coating is irradiated by laser, the temperature at the irradiation area on the coating is Gaussian distributed. The center of the irradiation area reaches the highest temperature. The largest change in the optical constants occurs in the center of the irradiated area, so a bulge will form during the irradiation of the laser pulse, which affects the optical properties of the coatings and the quality of the far-field beam. As shown in Fig. 9, the sample is the Au-SiO_2-Au coating. The thickness of Au layer is 45 nm, and that of SiO_2 layer is 30 nm. The wavelength of laser irradiating on the sample is 520 nm, the pulse width is 360 fs, the fluence is ~0.8 J/cm^2. The formation of the bulge proved the tensile stress formed during laser irradiation. The tensile stress results from the different change in the optical constants of the substrate and the coatings during the laser irradiation.

4.3. Defects formation at/near the interface of different coatings in the vacuum

As for the fact that the LIDT in the vacuum is obviously lower than that in the atmosphere [16], the difference of the changes of thickness and refraction index from atmosphere to vacuum results to stress and defects at the interface of coatings. Defects easily form in coatings in the vacuum, which makes coating easier be damaged by laser irradiation. As discussed above, when the pressure changes from the atmosphere to vacuum, the refractive index of SiO_2, and HfO_2 decreased by 2% and 1.6%, respectively, and the thickness changed by 3.4% and 0.3%, respectively. The different change of thickness and refraction index of coating layers cannot be ignored from atmosphere to vacuum, resulting to the stress at the interface and defects forming before the laser radiation, and organic contaminations which lowers the LIDT of coatings in the vacuum [43].

5. Conclusions

The refractive index and thickness of SiO_2 and HfO_2 single layer as a function of temperature were measured in the range from 23 °C to 320 °C. For all the layers, a rapid decrease at first and then a slow increase was observed for the refractive index, while the thickness of the layers first increased and then decreased. These results can be explained by the combination of water loss, densification and hydrophilicity in the films. The variation of the refractive index and thickness parameters of SiO_2 and HfO_2 single layer with temperature in the vacuum were measured to verify the proposed theory. These results help to understand the change of the coating during the laser damage process, to interpret the formation of transient defects based on the modification of the optical properties of coatings with temperature, and to explain the phenomenon that LIDT of coatings in the vacuum is lower than that in the atmospheric pressure.

Funding

National Key R&D Program of China (No. 2018YFE0115900); National Natural Science Foundation of China (61975220 and 61975219).

Declaration of competing interest

The authors declare that they have no known competing financial interests or personal relationships that could have appeared to influence the work reported in this paper.

Acknowledgments

We thank the National Natural Science Foundation of China and the National Key R&D Program of China for their financial contributions.

References

[1] H.B. He, H.Y. Hu, Z.P. Tang, Z.X. Fan, H.D. Shao, Laser-induced damage morphology of high-reflective optical coatings, Appl. Surf. Sci. 241 (3–4) (2005) 442–448.
[2] H. Wang, et al., Defect analysis of UV high-reflective coatings used in the high power laser system, Opt. Express 23 (4) (2005) 5213–5220.
[3] C. Yin, et al., HfO2/SiO2 anti-reflection films for UV lasers via plasma-enhanced atomic layer deposition, J. Alloys Compd. 859 (2021) 157875.
[4] J. Shao, K. Yi, M. Zhu, Thin-film polarizer for high power laser system in China, Int. Soc. Opt. Photon 9983 (2016) 998308.
[5] T.W. Walker, A.H. Guenther, P. Nielsen, Pulsed laser-induced damage to thin-film optical coatings-part II:Theory, IEEE J. Quantum Electron. 17 (10) (1981) 2053–2065.
[6] M.R. Kozlowski, I.M. Thomas, J.H. Campbell, et al., High-power optical coatings for a megajoule class ICF laser, The Lens Opt. Syst Design 1780 (1993) 105–119.
[7] J.S. Accetta, R.F. Shea, Sources of optical distortions in high energy laser systems, Proc. SPIE, the Int. Soc. Opt. Eng. 121 (1978) 132–139.
[8] M. Zhu, et al., Research on the laser damage performance of high reflection coatings at 355 nm, Proc. SPIE, the Internatioanl Society for Optical Engineering 8786 (2013) 87860X.
[9] M. Zhang, Z. Lu, Y. Pu, L. Lv, Z. Qiao, P. Ma, Investigation of the high repetition rate picosecond laser induced damage properties of dielectric reflective optical coatings, Proc. SPIE, Pacific Rim Laser Damage 2019: Optical Materials for High-Power Lasers 11063 (2019) 110630Z.
[10] X.F. Tang, Z.X. Fan, Z.J. Wang, Surface inclusion adhesion of optical coatings, Opt. Eng. 33 (10) (1994) 3406–3410.
[11] W.H. Lowdermilk, D. Milam, Laser induced surface and coating damage, IEEE J. Quantum Electron. 17 (9) (1981) 1888–1903.
[12] M. Lequime, et al., Laser-induced damage of pure and mixture material high reflectors for 355 nm and 1064 nm wavelength, Proc. SPIE, Advances in Optical Thin Films IV 8168 (2011) 816821.
[13] L. Gallais, M. Commandre, Laser-induced damage thresholds of bulk and coating optical materials at 1030 nm, 500 fs, Appl. Opt. 53 (4) (2014) A186-96.
[14] B. Mangote, et al., A high accuracy femto-/picosecond laser damage test facility dedicated to the study of optical thin films, Rev. Sci. Instrum. 83 (1) (2012) 013109.
[15] L.N. Taylor, A.K. Brown, A.J. Pung, E.G. Johnson, J.J. Talghader, Continuous-wave laser damage of uniform and nanolaminate hafnia and titania optical coatings, Opt. Lett. 38 (21) (2013) 4292–4295.
[16] A.K. Burnham, M.J. Runkel, S.G. Demos, M.R. Kozlowski, P.J. Wegner, Effect of vacuum on the occurrence of UV-induced surface photoluminescence, transmission loss, and catastrophic surface damage, Proc. SPIE, the International Society for Optical Engineering Symposium on Optical Science and Technology 4134 (2000) 243–252.
[17] J.R. Jacobsson, J.R. Palmer, Theoretical model for evaluating transient temperature distribution in rugate optical thin film coatings subject to high power continuous wave and repetitive pulsed lasers, Proc. SPIE, Thin Film Technologies II 652 (1986) 284–294.

[18] M.R. Kozlowski, R. Chow, Role of defects in laser damage of multilayer coatings, Proc. SPIE, Laser-Induced Damage in Optical Materials 2114 (1994) 640–649.
[19] D. Ristau, M. Jupé, K. Starke, Laser damage thresholds of optical coatings, Thin Solid Films 518 (5) (2009) 1607–1613.
[20] S. Ohkubo, K. Aoki, D. Eto, Temperature dependence of optical constants for InSb films including molten phases, Appl. Phys. Lett. 92 (1) (2008).
[21] F. Aousgi, W. Dimassi, B. Bessais, M. Kanzari, Effect of substrate temperature on the structural, morphological, and optical properties of Sb2S3 thin films, Appl. Surf. Sci. 350 (2015) 19–24.
[22] Z.H. Duan, Z.G. Hu, K. Jiang, et al., Temperature-dependent dielectric functions and interband critical points of relaxor lead hafnate-modified PbSc1/2Ta1/2O3 ferroelectric ceramics by spectroscopic ellipsometry, Appl. Phys. Lett. 102 (15) (2013) 224105-R.
[23] T. Jung Kim, et al., Temperature dependence of the dielectric functions and the critical points of InSb by spectroscopic ellipsometry from 31 to 675 K, J. Appl. Phys. 114 (10) (2013) 114516-1077.
[24] A. Dejneka, et al., Spectroscopic ellipsometry applied to phase transitions in solids: possibilities and limitations, Opt. Express 17 (16) (2009) 14322–14338.
[25] D. Hrabovsky, et al., Strontium titanate (100) surfaces monitoring by high temperature in situ ellipsometry, Appl. Surf. Sci. 367 (2016) 307–311.
[26] A. Paone, R. Sanjines, P. Jeanneret, A. Schüler, Temperature-dependent multiangle FTIR NIR–MIR ellipsometry of thermochromic VO2 and V1-w O2 films, Sol. Energy 118 (2015) 107–116.
[27] M.L. Grilli, F. Menchini, A. Piegari, D. Alderighi, G. Toci, M. Vannini, Al2O3/SiO2 and HfO2/SiO2 dichroic mirrors for UV solid-state lasers, Thin Solid Films 517 (5) (2009) 1731–1735.
[28] Y.S. Jung, Spectroscopic ellipsometry studies on the optical constants of indium tin oxide films deposited under various sputtering conditions, Thin Solid Films 467 (1–2) (2004) 36–42.
[29] Y. Shan, et al., Measuring optical constants of ultrathin layers using surface-plasmon-resonance-based imaging ellipsometry, Appl. Opt. 56 (28) (2017) 7898–7904.
[30] A.A. Perrotta, Looking down the rabbit hole: nano-porosity in thin films, Door Alberto Perrotta (2016).
[31] D.I. Kushner, M.A. Hickner, Water sorption in electron-beam evaporated SiO2 on QCM crystals and its influence on polymer thin film hydration measurements, Langmuir 33 (21) (2017) 5261–5268.
[32] C. Vallee, A. Goullet, A. Granier, Direct observation of water incorporation in PECVD SiO2 films by UV–Visible ellipsometry, Thin Solid Films 311 (1–2) (1997) 212–217.
[33] A. Goullet, C. Vallée, A. Granier, G. Turban, Optical spectroscopic analyses of OH incorporation into SiO2 films deposited from O2/tetraethoxysilane plasmas, J. Vac. Sci. Technol. A: Vacuum, Surfaces, and Films 18 (5) (2000) 2452-2358.
[34] H.A. Macleod, Structure-related optical properties of thin films, J. Vac. Sci. Technol. A: Vacuum, Surfaces, and Films 4 (3) (1986) 418–422.
[35] D.B. Asay, S.H. Kim, Evolution of the adsorbed water layer structure on silicon oxide at room temperature, J. Phys. Chem. B 109 (35) (2005) 16760–16763.
[36] S.S. Lin, C.S. Liao, The hydrophobicity and optical properties of the HfO2-deposited glass, Ceram. Int. 39 (1) (2013) 353–358.
[37] T. Jitsuno, et al., Source of contamination in damage-test sample and vacuum, in: Proc. Pacific Rim Laser Damage 2016, Optical Materials for High-Power Lasers 9983 (2016) 998316.
[38] S.K. Parida, S. Dash, S. Patel, B.K. Mishra, Adsorption of organic molecules on silica surface, Adv. Colloid Interface Sci. 121 (1–3) (2006) 77–110.
[39] Y. Cui, S.J. Liu, H.B. He, et al., Influence of vacuum organic contaminations on laser-induced damage of 1064 nm anti-reflective coatings, Chin. Phys. Lett. 24 (10) (2007) 2873–2875.
[40] M. Verghese, E. Shero, F. Shadman, Multicomponent interactions of moisture and organic impurities with the wafer surface, in: Proc. Symposium on Electrochemical Processing in ULSI Fabrication I at the 193rd Meeting of the Electrochemical-Society, vol. 98, 1998, pp. 112-121.
[41] Y. Luo, et al., Laser-induced bulk modification in KDP crystal analyzed by optical spectroscopy under high-power laser excitation, J. Lumin. 207 (2019) 236–240.
[42] C.S. Liu, N. Kioussis, S.G. Demos, H.B. Radousky, Electron- or hole-assisted reactions of H defects in hydrogen-bonded KDP, Phys. Rev. Lett. 91 (1) (2003) 015505.
[43] X.L. Ling, et al., Effect of vacuum on the laser-induced damage of anti-reflection coatings, Chin. Phys. Lett. 26 (7) (2009) 074203.